Sensitive Force Technique to Probe Molecular Adhesion and Structural Linkages at Biological Interfaces

E. Evans, K. Ritchie, and R. Merkel
Departments of Physics and Pathology, University of British Columbia, Vancouver, British Columbia, Canada V6T 1W5

ABSTRACT Adhesion and cytoskeletal structure are intimately related in biological cell function. Even with the vast amount of biological and biochemical data that exist, little is known at the molecular level about physical mechanisms involved in attachments between cells or about consequences of adhesion on material structure. To expose physical actions at *soft* biological interfaces, we have combined an ultrasensitive transducer and reflection interference microscopy to image submicroscopic displacements of probe contact with a test surface under minuscule forces. The transducer is a cell-size membrane capsule pressurized by micropipette suction where displacement normal to the membrane under tension is proportional to the applied force. Pressure control of the tension tunes the sensitivity in operation over four orders of magnitude through a range of force from 0.01 pN up to the strength of covalent bonds (~1000 pN)! As the surface probe, a microscopic bead is biochemically *glued* to the transducer with a densely-bound ligand that is indifferent to the test surface. Movements of the probe under applied force are resolved down to an accuracy of ~5 nm from the interference fringe pattern created by light reflected from the bead. With this arrangement, we show that local mechanical compliance of a cell surface can be measured at a displacement resolution set by structural fluctuations. When desired, a second ligand is bound sparsely to the probe for focal adhesion to specific receptors in the test surface. We demonstrate that monitoring fluctuations in probe position at low transducer stiffness enhances detection of molecular adhesion and activation of cytoskeletal structure. Subsequent loading of an attachment tests mechanical response of the receptor-substrate linkage throughout the force-driven process of detachment.

INTRODUCTION

Adhesion between soft interfaces is an important phenomenon in many fields of science and technology. What scientists would like to know about adhesion and surface structure depends on professional interests. In biology, the objectives are to describe the consequences of intercellular attachment on the biochemistry and function of cells. In physics, the objectives are to relate submicroscopic actions of bond formation and rupture to molecular structure and fields. To coalesce these objectives, physical probes are needed that will expose single bonds under load and test material properties of molecular structures in liquids over a force range of 0.01–1000 pN. The wide range of force arises because adhesive ligands in biology form many types of bonds to surface receptors, and these receptors are linked in many different ways to the interfacial structure (Bell, 1978; Springer, 1990; Evans, 1994). On a quantitative scale, strengths of weak noncovalent bonds (e.g., hydrogen and van der Waals) are expected to be in the range of 10–100 pN. Surprisingly, even weaker forces below 10 pN have been found in biocellular systems (e.g., myosin/actin and kinesin *motor* tractions ~1 pN) (Ashkin et al., 1990; Ishijima et al., 1991; Kuo and Sheetz, 1993). Likewise, mechanical susceptibilities of biointerfacial structures span a large range in force, e.g.: <0.1 pN force will significantly extend a surface-grafted polymer or displace a membrane under low tension; a force of ~20 pN is sufficient to extract a lipid-anchored receptor (Evans et al., 1991), but a force in excess of 100 pN is needed to stretch an actin filament to its breaking point (Kishino and Yanagida, 1988). An important consequence of ultrasoft interfaces in biology is that surface topography is rough and lacks precise definition. Thus, there is no need to seek fine positional resolution of the interface below a level of 10 nm or more set by macromolecular structure and thermal fluctuations. Instead, the aim is to resolve forces from the extremely small to the limit of molecular strength with minimal perturbation to the native structure.

Several methods have been developed to measure weak interactions between surfaces on the submicroscopic scale. In the study of colloid interactions, a major advance has been the surface force apparatus SFA (Israelachvili and Adams, 1978; Parker et al., 1989). This innovation has enabled measurements of uniform attractive and repulsive fields between cm-size smooth surfaces at distances from 1 to 100 nm. After widespread application to colloid interactions (Israelachvili and Pashley, 1982, 1983; Luckham and Klein, 1985), recent investigations have included attraction between Langmuir-Blodgett bilayers (Marra and Israelachvili, 1985) and fracture of molecularly bonded bilayers (Leckband et al., 1992). Although very useful for study of smooth surfaces on a large scale, it is difficult to use SFA for study of focal interactions between biological cells. By comparison, development of the atomic force microscope AFM (Binnig et al., 1986) has shown that classical methods can image invisible textures and mechanical properties of local molecular structures. AFM technology is advancing rapidly with applications to many areas of science and technology (Drake et al., 1989;

Received for publication 26 October 1994 and in final form 16 February 1995.

Address reprint requests to Dr. Evan Evans, Department of Pathology, University of British Columbia, 2211 Wesbrook Mall, Vancouver, BC, V6T 1W5. Tel.: 604-822-7103; Fax: 604-822-7635.

0006-3495/95/06/2580/08 $2.00

Maivald et al., 1991). The concept is based on a simple cantilever beam design where the tip deflection is proportional to the force. Several aspects mark advances in this technology, but the most relevant feature is the force sensitivity — given by the cantilever stiffness k_f = force/deflection. Early versions of AFM were characterized by stiffnesses of many N/m requiring forces of at least 1000 pN for *atomic* (0.1 nm) deflections. Such levels of force are comparable with the strength of weak covalent or ionic bonds. With *state-of-the-art* micromachining, the most sensitive versions of AFM today have stiffnesses of order 1 mN/m and have been used to detect single hydrogen bonds (Hoh et al., 1992). Using soft cantilevers, a recent thrust in AFM has been imaging biological structures from lipid bilayers (Zasadzinski et al., 1991) to biomolecules (Radmacher et al., 1992) and probing biomolecular bonds (Lee et al., 1994). Other sensitive methods include observation of trajectories of two attached-spherical particles in a fluid shear field (van de Ven and Mason, 1976; Tha and Goldsmith, 1986; Tha et al., 1986; Tees et al., 1993) and displacement of a microbead probe held in a laser-optical trap (Ashkin, 1992). However, because of the more distributed nature of forces and more complicated physics, the fluid shear and optical tweezer methods have not been applied as widely as the mechanical SFA and AFM techniques.

To probe easily molecular adhesion and structure at living cell interfaces, we have developed a simple transducer that provides both the capability to measure the full range of force from 10^{-2} to 10^3 pN *and* the appropriate mechanical stiffness to match the soft mechanical compliance of cell surfaces. We originally devised this method to test strengths of molecular attachments formed between red cells by specific agglutinins (Evans et al., 1991). We found that the rupture forces were astonishingly small, 20–30 pN, which demonstrated the need for an ultrasensitive technique. Motivated by SFA and AFM technology, we have assembled the transducer into a versatile apparatus that provides submicroscopic control of transducer position and nanoscale resolution of the probe interaction with a test surface. Here we describe the important elements of the system arranged to probe horizontal surfaces where the transducer is moved along a vertical trajectory. (We have also assembled a version for testing vertical surfaces (e.g., surfaces of suspended cells) that will be discussed in a future paper.) Our main objective is to demonstrate prototypical procedures for testing molecular adhesion to, and local mechanical compliance of, surface films or tissue culture cells.

BIOINTERFACE PROBE: APPARATUS AND EXPERIMENTAL METHODS

Force transducer and surface probe

The force transducer is a membrane capsule pressurized by micropipette suction to which a microbead is *glued* to create a surface probe. Convenient choices for the capsule are mammalian red blood cells and synthetic lipid bilayer vesicles; examples are shown in Fig. 1. Capsule pressurization is precisely controlled by micropipette suction P (1 μatm to 0.1 atm) which, thereby, sets the membrane tension τ_m. Small axial forces applied to the bead extend (+) or compress (−) the spherical shape of the capsule by a small displacement Δz proportional to the force f (see Fig. 1); the stiffness $k_f = f/\Delta z$ of the transducer is defined by the capsule membrane tension τ_m. Thus, the sensitivity to force can be varied over four orders of magnitude (i.e., 1 μN/m < k_f < 10 mN/m) by merely changing the suction pressure; no other calibration is required. As we will show, probe displacements can be measured down to values of a few nm, so forces below 0.1 pN can be detected! In general, the lower bound for force detection is determined by both resolution of transducer deflection and thermal fluctuations scaled by $\Delta f^2 \sim k_B T \cdot \tau_m$. At the lowest level of tension, fluctuations limit minimum forces to the order of 0.1 pN because $k_B T \sim 4 \times 10^{-21}$ N-m. Likewise, at this level of stiffness, fluctuations in probe position are of order $\Delta z_b^2 \sim k_B T/\tau_m > |10\ \text{nm}|^2$. Later, we will show that measurements of fluctuations in probe position versus membrane tension confirm these simple relations for 1-D harmonic excitations.[1]

To examine a wide variety of biosurfaces and adhesion complexes, a versatile probe is needed. For this component, we have chosen polystyrene latex microbeads (~2–3 μm diameter) conjugated with surface-reactive aldehyde groups (acrolein-derivatized polystyrene latex, Interfacial Dynamics, Portland, OR). The microbead is first densely bound with a ligand *glue* that is indifferent to the test surface but sticks the probe strongly to the transducer membrane. (Examples include blood group-specific IgG antibodies or lectins for bonding to red cell capsules and monoclonal anti-dinitrophenyl DNP IgG or streptavidin for bonding to lipid bilayer capsules doped with 1% DNP-phosphatidyl choline or biotinylated phosphatidyl ethanolamine.) If adhesion is to be tested, the bead is next bound sparsely with a second ligand for focal attachment to receptors in the test surface. To isolate molecular adhesion sites, the density of the ligand specific to the surface receptor is reduced to a level (<100/μm^2) where point contact between the probe and the test surface produces infrequent discrete attachments. As docking sites for specific adhesive ligands, a simple approach is to bind a low density of streptavidin proteins to the probe and then attach a biotinylated ligand (*Avidin-Biotin Chemistry: A Handbook*, Pierce Chemical, Rockford, IL). (Chemical procedures for coupling these ligands to the probe are described in detail in a manuscript by Tha, Leung, Ritchie, Narla, and Evans, to be submitted.) After chemical preparation, a suspension of beads is placed in an isolated region of the microscope chamber at very low concentration. Selected by pipette suction from another region of the microchamber, a membrane capsule is maneuvered into position above a bead on the coverglass floor of the chamber. Then, by piezo control of the pipette, the membrane capsule is pushed against the bead. The result is strong adhesion of the bead to the capsule membrane over a macroscopic area of contact as shown in Fig. 1.

[1] Prescriptions for capsule stiffness depend on material characteristics of the membrane. For fluid membrane behavior (e.g., lipid bilayers with fluid acyl chains and red cell membranes at tensions in excess of the surface shear modulus, i.e., $\tau_m \geq 10^{-2}$ mN/m), tension is uniform over the capsule surface and given by

$$\tau_m = P \cdot R_p/2(1 - R_p/R_o),$$

where R_p and R_o are the pipette radius and outer capsule radius, respectively (Evans and Skalak, 1980). Similarly, the capsule deformation under a small axial force can be readily analyzed because the unsupported shape of the membrane is a surface of constant mean curvature (Evans and Skalak, 1980). Performing the required integration, first approximation to the stiffness is found to be

$$k_f \approx 2\pi \cdot \tau_m/[\ln(2R_o/R_p) + \ln(2R_o/r_b)],$$

where r_b is the circular radius of the adhesive contact between the microbead and capsule membrane (Evans et al., 1991). With typical geometries of transducers, $k_f \sim 2\ \tau_m$.

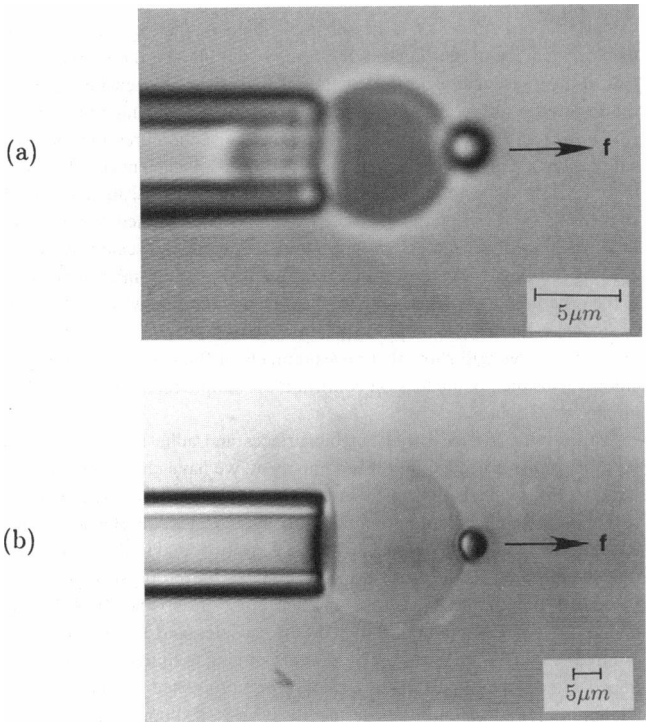

FIGURE 1 Videomicrographs of membrane capsules used as picoforce transducers: (*a*) A human red blood cell (outside spherical diameter ~6 μm); and (*b*) a phospholipid bilayer vesicle (diameter ~20 μm). In each case, a solid-latex microbead was biochemically *glued* to the capsule membrane by ligands covalently bound to the bead (e.g., an antibody specific to the red cell blood group and a monoclonal antibody to DNP phospholipids doped in the vesicle bilayer). Displacement Δz of the bead along the axis of the transducer is proportional to the force f, i.e., $\Delta z \sim f/\tau_m$, where τ_m is the membrane tension set by pipette suction pressure.

Optical detection and control of submicroscopic displacements

To expose submicroscopic interactions of the probe with a horizontal test surface, an inverted-vertical microscope (Zeiss *Axiovert*) was fitted with reflection interference contrast optics (Zeiss *Antiflex* Neofluar 63 ×/1.25 NA oil immersion) to image the probe above the test surface. The interference pattern produced by light reflected from the microbead encodes the elevation above the coverglass (Zilker et al., 1992; Radler and Sackmann, 1992). A second specially designed horizontal microscope was constructed to provide a lateral view of the force transducer. This *sideways* perspective facilitates initial assembly of the microbead to the transducer capsule and manipulation over the test surface. Movement of the transducer to/from the test surface is controlled by a piezoelectric element (5 μm travel stacked piezo, Physik Instruments, Waldbronn, Germany) mounted in series with mechanical microtranslation of the transducer pipette. (The complete schematic of the assembly is shown in Fig. 2.) To determine probe position, dedicated image analysis software is used to compute circularly averaged radial sections of each fringe pattern at video framing rates (30/s). Then, based on the fixed spherical geometry of the microbead probe, fringe intensity fields are predicted and matched to the radial section of each video fringe pattern through variation of bead elevation above the coverglass. By this method, probe positions along the optical axis can be resolved to better than 5 nm; lateral resolution in the position of the bead is of order 10–15 nm. In Fig. 3, data show the correlation between piezo-driven displacements Δz_t and positions z_b of a microbead held directly by micropipette over the course of repeated excursions to/from the coverglass surface.

Reflection properties of an intervening cell on the coverglass weakly modulate the fringe pattern produced by the probe. The effect is shown in Fig. 4 for a probe positioned at various locations on the top surface of a tissue culture cell spread on the coverglass. (Note that the tissue culture cells used in the prototype tests were an immortalized line of hamster kidney BHK cells kindly provided to us by Dr. J. Piret of the Biotechnology Laboratory, University of British Columbia.) Even with some fringe degradation, probe *movements* are still resolvable to a few nanometers. This level of resolution is possible because there is strong reflection from the fixed spherical contour of the probe *and* the optical phase encoded in the pattern depends on the absolute refractive index and total path length between the probe and coverglass — not the differential value of refractive index relative to water. (Note that the average index of refraction for most cells lies between 1.33 (water) and 1.40 (e.g., the highly refractile red blood cell) as compared with ~1.55 for glass.) After digitization of the video field, the reference background field can be subtracted if desired as illustrated in Fig. 4 (this step seldom is needed for weakly refractile cells). Next, the center of the fringe pattern is computed accurately, and the pattern is averaged circularly to obtain a radial section. The latter step has the effect of averaging multiple images in one field, which significantly suppresses random intensity variations and video noise in the computed image. To demonstrate the approach, circularly averaged fringe patterns found by software analysis are plotted in Fig. 4 adjacent to the direct video images. Optimal fits and the computed values of bead elevations above the coverglass are superposed on the radial sections in Fig. 4; also, variations predicted by ±5 nm deviations in bead elevation are added to illustrate resolution. The practical limit for cell thickness between the probe and coverglass is set by the coherence length of the microscope Hg light source (a few μm).

Environment for prototype tests

In all of the prototype tests to be described next, red blood cells were used as transducer capsules. These cells were obtained from finger-prick blood samples suspended in 0.07 M NaCl buffers (either phosphate or HEPES, pH 7) plus 0.5% by weight BSA to prevent adhesion of the cell capsule to the holding pipette.

RESULTS OF PROTOTYPE TESTS

Probe fluctuations, soft surface contact, and nonspecific adhesion

Transducer sensitivity and force resolution are demonstrated in Fig. 5 by measurements of fluctuations in probe position along the optical axis at various levels of transducer stiffness. The results show that mean-square fluctuations in position vary inversely with the level of tension applied to the capsule membrane by pipette suction. The linear fit to the data is consistent with the simple relation for 1-D harmonic excitations introduced earlier, $\Delta z_b^2 \sim k_B T/\tau_m$. The dynamic roughness illustrated in Fig. 5 not only demonstrates how fluctuations affect force detection but, more generally, how fluctuations superpose on intrinsic macromolecular texture at soft cell interfaces to compromise resolution of molecular structure.

At low transducer stiffness, fluctuations in probe position provide a very useful diagnostic to achieve gentle contact with a test surface. When contact is made with a surface, the fluctuations diminish precipitously as a consequence of the stiffness contributed by the interface. The low transducer stiffness also increases sensitivity to long-range attraction between the probe and the surface (e.g., nonspecific van der Waals forces). If long range attraction is significant, *jump* to contact ensues that has been well documented in studies of colloid interactions using SFA (Israelachvili and Adams,

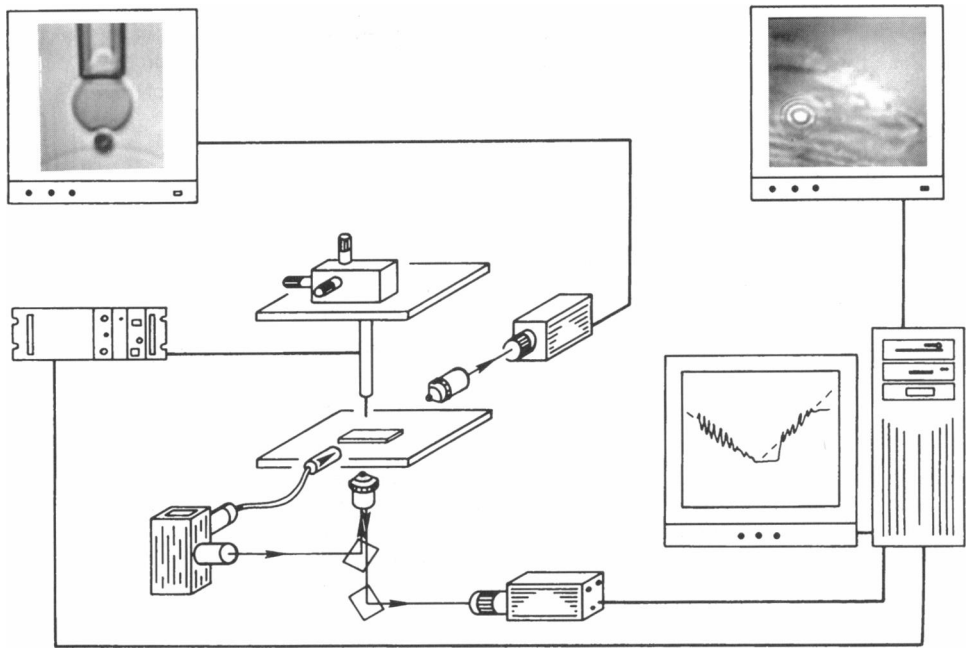

FIGURE 2 Schematic of the biointerface probe apparatus. Orthogonal microscopes image both the submicroscopic movements of the microbead probe to/from a coverglass substrate (the inverted microscope with reflection interference contrast optics) and macroscopic maneuvers of the transducer over the test surface (the horizontal microscope). A piezoelectric element accurately controls approach to/from the test surface. A dedicated computer directs the nanoscale translation of the transducer and simultaneously analyzes the elevation of the probe above the coverglass from the interference image.

1978; Israelachvili and Pashley, 1982, 1983; Parker et al., 1989). Examples are shown in Fig. 6 for jump to contact through weak nonspecific attraction and soft contact with no apparent attraction. These tests were carried out in 0.07 M NaCl plus albumin, and the probe was conjugated with only a transducer *glue* indifferent to the coverglass coated by the serum albumin. Through the stiffness constant of the capsule transducer (i.e., membrane tension), the differential displacement $\Delta(z_t - z_b)$ between transducer and probe positions specified the repulsive and attractive forces of interaction with the surface. From the data for probe force versus transducer position, we see that both long range attraction (−) and impingement (+) at soft contact involved extremely small

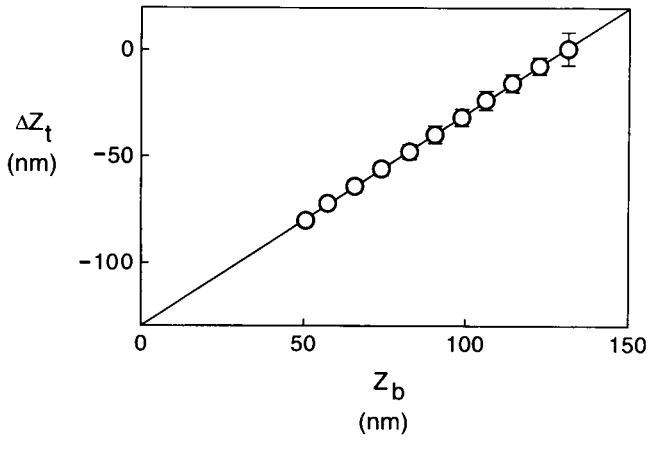

FIGURE 3 Experimental correlation of piezo-driven translation Δz_t of a microbead held by a micropipette and positions z_b of the bead above the coverglass. The pipette was moved repeatedly in the direction to/from the coverglass surface. Positions of the bead above the coverglass were computed from a complete fit to a circularly averaged radial section of each video interference image; sizes of the open circles are comparable with resolution of probe positions.

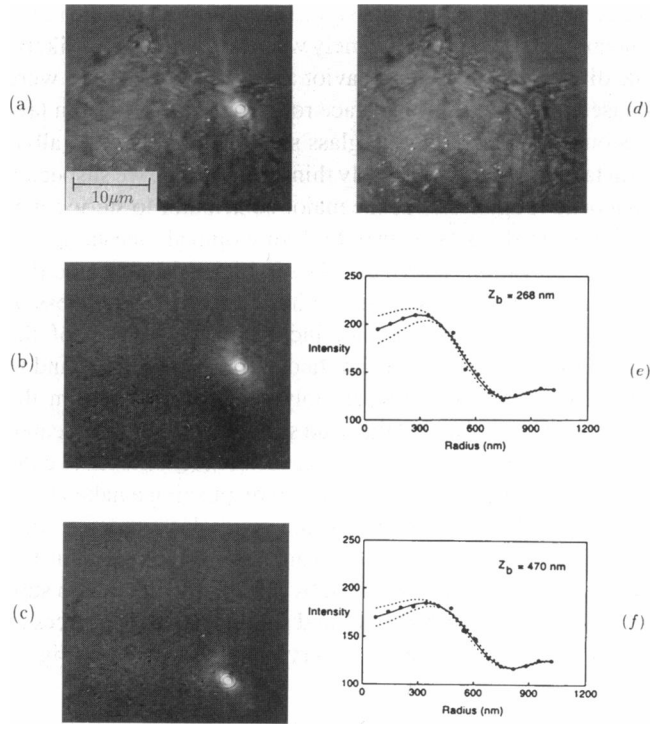

FIGURE 4 Video micrographs (*a-c*) of a probe placed in contact with the upper surface of a BHK tissue culture cell spread on the coverglass (*d*, before probe contact). *b* and *c* show the probe image at two locations after the background reference image (*d*) was subtracted. Circularly averaged radial sections of the probe interference patterns are shown in *e* and *f* as derived by computer image analysis. Superimposed on these radial sections are optimal fits (——) that yielded elevations (*inset*) of the probe above the coverglass at each location. Also, predictions of fringe intensities for ±5 nm deviations in elevation are added (- - - -) to illustrate distance resolution.

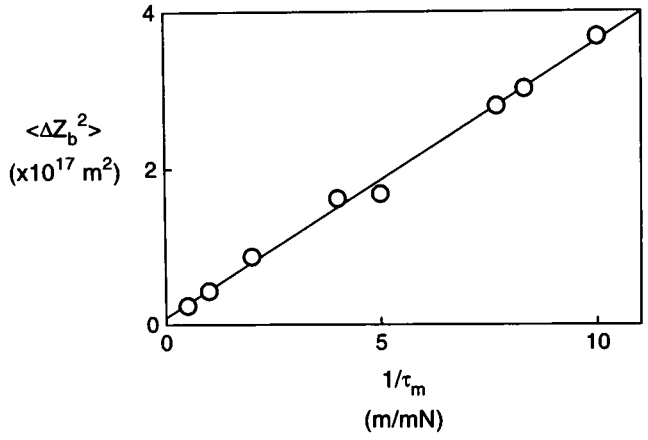

FIGURE 5 Measurements of mean-square fluctuations Δz_b^2 in probe position along the optical axis versus reciprocal tension $1/\tau_m$ applied to the transducer membrane. As expected for simple 1-D harmonic excitations, the slope of the data is $\sim 3.7 \times 10^{-21}$ J, which is close to the value of thermal energy k_BT at room temperature.

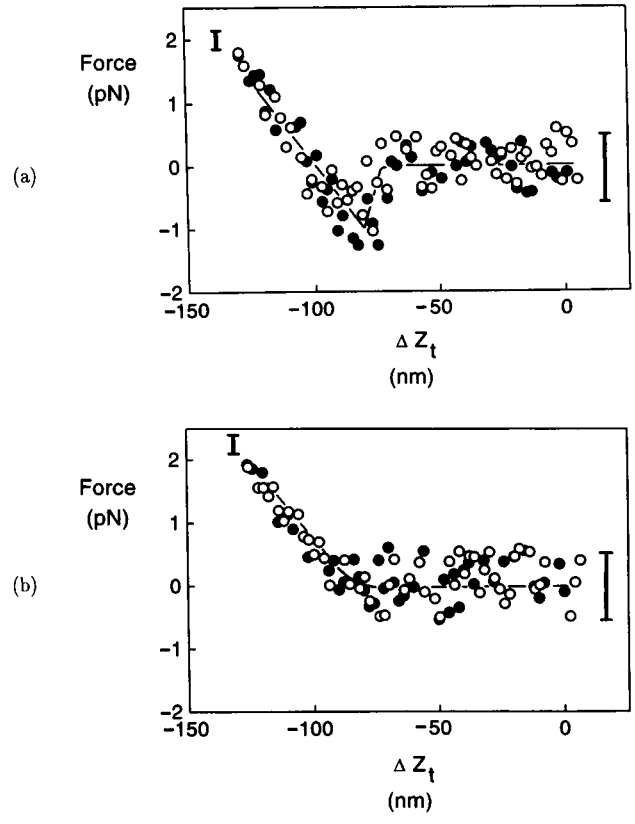

FIGURE 6 Ultrasensitive detection of nonspecific probe interactions with an albumin-coated glass test surface. The running average of the force (——) is plotted versus transducer displacement Δz_t; also, ~10% of the data points within ±1 SD (shown by *vertical bars*) of the average are superposed to demonstrate suppression of fluctuations on *soft* contact with the surface. (●, Approach to (○, withdrawal from) the surface.) In *a*, a sharp negative step in force signaled a jump to surface contact driven by long range van der Waals attraction that reversed on separation. However, as seen in *b*, often contact with the surface showed no evidence of long range attraction.

forces — less than 1 pN! (Note that following the nomenclature of AFM, compressive forces are taken as positive and tensile forces of attachment are defined as negative.) Because van der Waals attraction is always present, the probe should always jump to contact in physiological solutions of ~0.1 M electrolyte (NaCl). However, as demonstrated by the examples in Fig. 6, there were significant variations in the range and magnitude of this extremely weak attraction. Most likely, the differences in jump behavior and level of attraction were caused by variations in surface roughness of the protein layers on the probe and coverglass surfaces. Because the albumin layer should be relatively thin and uniform, we suspected that bead roughness was the major contributor to steric separation from the glass substrate. Using optical measurements of bead elevations above the glass in high salt, we found that the naked latex beads appear to have a surface roughness of 42 ± 3 nm, which was not increased by addition of the protein components. This implied that the proteins bound to the bead in valleys between polymer projections from the bead surface. (Note that the bead surface roughness appeared to represent a compliant *fuzz* because the elevation above the coverglass could be reduced to zero by pushing a naked bead directly with a pipette toward the coverglass under a large force.) Simple calculation of van der Waals attraction between a latex sphere separated by ~40 nm from a glass substrate yielded jump distances and small detachment forces of ~1 pN consistent with the observations illustrated in Fig. 6.

Cell surface roughness and mechanical compliance

The compliance and roughness of a living cell interface are demonstrated in Fig. 7 by the force response sensed when the probe was driven into the thin lamellar periphery of a BHK cell spread tightly on the coverglass. Contact with the cell interface was signaled by a step in force at a probe elevation $z_b \sim 260$ nm above the coverglass (Fig. 7 *a*). However, as seen, the rise in force covered 10–15 nm, which implied that the breadth of the interface was threefold greater than the resolution in probe position. To test compliance of the cell cortex below the interface, the probe was pushed further into the cell at a rate of ~30 nm/s and, the compressive force was registered again by the differential displacement $\Delta(z_t - z_b)$ between transducer and probe positions. After large indentation of the interface with little increase in compressive force, the cell structure stiffened to resist forces of nearly 1 nN and exhibited small variations indicative of material inhomogeneities. When the transducer was retracted, the force returned to zero without attachment to the surface but pronounced hysteresis exposed viscous damping in the cytostructure (Fig. 7 *b*). The ratio of surface indentation to the probe radius showed that a small region of <1 μm in size was probed in the compression test. As contact between the bead and cell surface increased, more components of the cell structure opposed compression and produced irregularities in the force response, as seen in Fig. 7. Using the average area of contact derived from the indentation, the maximum level of force in Fig. 7 converts to apparent values on order of 400 N/m^2 ($\sim 4 \times 10^{-3}$ atm) for compressive stress, which dem-

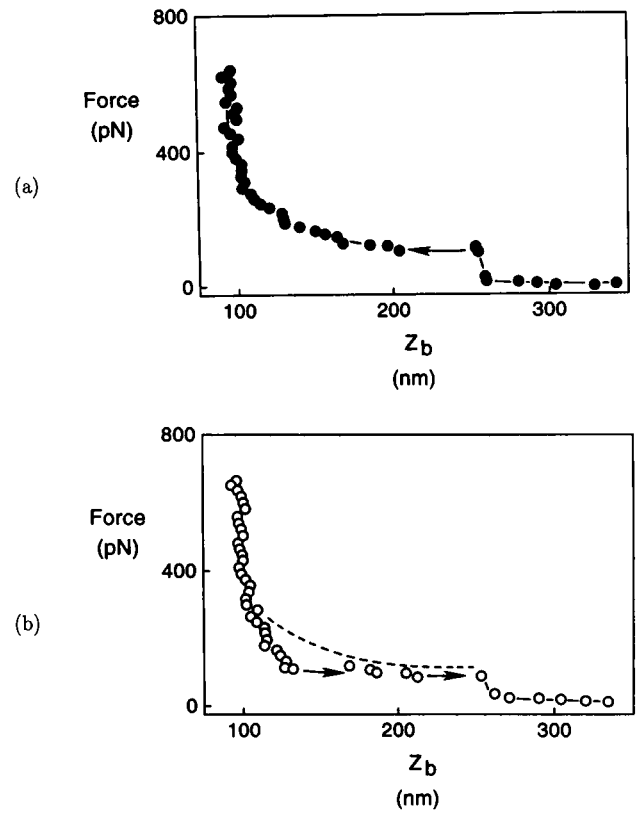

FIGURE 7 Compliance of a BHK cell interface as measured by force f versus probe position z_b. In the upper figure, the probe was driven into contact with the surface of the tissue culture cell spread on the coverglass at a rate of ~30 nm/s. The running average of the force data is plotted as the data points. The size of the circles is comparable with the optical resolution. Note in *a* that the probe force rose steeply on contact with the cell interface at a separation of $z_b \sim 260$ nm and showed a breadth of ~10–15 nm, indicative of surface roughness. Based on probe diameter and depth of progressive indentation, the compressive forces represented loading over a small region (<1 μm) of the cell surface. In *b*, forces are plotted for unloading at the same rate (○) with the loading response superposed as the dashed curve. The hysteresis exposed viscous fluid-like properties of the cell cortex in this thin lamellar region.

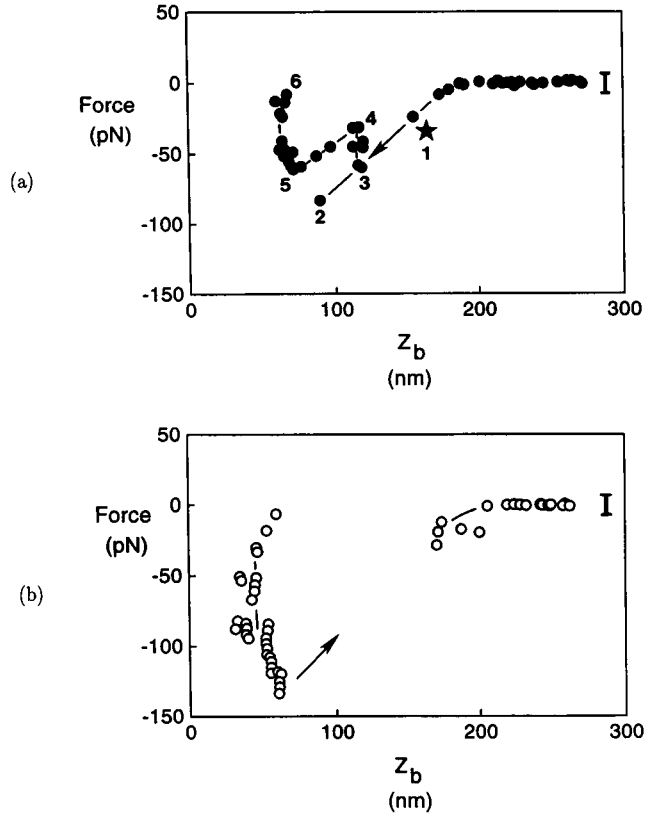

FIGURE 8 Specific adhesion to a BHK tissue culture cell produced by succinyl con A conjugated to the probe. In *a*, probe force is plotted for approach to the cell surface as a function of probe position. Unexpectedly, on attachment (noted by the *star*), the receptor was dynamically retracted by the subsurface cell structure as shown by the erratic force pulling on the probe. (Evolution of the cell response is noted by the numerical sequence 1-2-3-4-5-6.) The transducer was continued toward the cell in an attempt to null the attraction. After the retraction force on the attachment subsided, the transducer was withdrawn from the surface until the attachment ruptured as shown by the precipitous jump (*arrow* in *b*). The data for force versus probe position z_b before rupture exposed the mechanical stiffness of the receptor-interface linkage modulated by some cell-driven activity.

onstrated the soft character of the cell cytostructure in the thin lamellar periphery.

Bond formation and attachment strength

Weak nonspecific attraction and soft contact with the test surface enable very sensitive detection of adhesive bond formation. To demonstrate molecular bonding, the probe was sparsely conjugated with a second ligand (succinyl con A) for specific attachment to a BHK cell surface. (For these tests, the environmental solution was HEPES-buffered, glucose-free Hank's.) As shown in Fig. 8 *a*, formation of a con A attachment was accompanied often by dynamic retraction of the receptor by the cell. This unexpected feature was immediately obvious because the cell actually pulled on the bead, extending the transducer, even as the transducer was moved toward the surface to relax the force. Also, the cell retraction force applied to the probe was erratic until the transducer had been moved by >100 nm toward the cell. (Although the cell actively pulled on the probe immediately after succinyl con A attachment in many cases, there were tests where this was not detected.) When the cell retraction subsided, the attachment was stressed mechanically to rupture by withdrawing the transducer, as shown in Fig. 8 *b*. The small displacement of the probe over the course of increasing force (~30 pN/s) imaged the mechanical compliance of the ligand-receptor-interfacial linkage and again showed some cell-driven variations. Rupture of the attachment was detected immediately when the force disappeared and the probe recoiled from the cell surface. The maximum force at separation in Fig. 8 *a* defined the attachment strength, which was two orders of magnitude greater than the nonspecific forces described in the previous section. In a complete study, the dependence of rupture strength on loading rate must be determined to unravel the dynamics governing failure of a single molecular attachment (Evans and Ritchie, 1994). We have used this approach recently to examine the dynamic

properties of failure for biotin-conjugated probe attachments to streptavidin monolayers immobilized on coverglass substrates (Merkel et al., 1995). The rate of loading of attachments is varied by withdrawing the transducer from the surface at different rates. The upper bound on loading rate is set by the video-framing speed (30/s), whereas thermal drifts of the apparatus are expected to restrict slow loading of attachments to a duration of a several minutes.

CONCLUSIONS

We have described a simple apparatus and procedures for probing submicroscopic forces at biological interfaces. An important feature of the design is that transducer sensitivity can be tuned in operation to measure a wide range of force from 0.01 to 10^3 pN. For uniform interactions between the spherical probe and the test surface, our apparatus functions as a microscopic version of the SFA instrument developed by Israelachvili and others. On the other hand, if the microbead is studded with prominent macromolecules or colloidal-size (~10 nm) particles, a submicroscopic projection from the bead surface becomes the effective probe and interacts with a test surface like an AFM. In contrast to these established techniques, our chemically conjugated probe is not *atomically* smooth like the mica surfaces of an SFA, and our resolution of probe movements is not as good as that for a stiff AFM. Even so, there is no need to have *atomically* smooth probes or to seek ultrafine positional resolution at soft biological interfaces because these surfaces are made extremely rough by macromolecular structure and thermal fluctuations. As shown in the tests of interface compliance for a tissue culture cell spread tightly on glass, resolution of probe positions by conventional optical methods at a limit of ~5–10 nm is better than definition of the cell interface. A very useful feature of our force probe is that it is easy to find and softly touch a cell surface; thus, perturbations to cell structures can be minimized, and weak adhesive bonds can be detected readily. Furthermore, the sensitivity enables detection of local activation of cytoskeletal structure that may occur as a consequence of ligand binding to a single surface receptor. As with any of the force probes (SFA, AFM, particle disjoining in fluid shear, or optical *tweezers*), the most illusive aspect is control of the probe surface chemistry to either be indifferent, or bind specifically, to the test surface as desired. Care must be taken to ensure that biological ligands are covalently bonded to the probe surface without physisorbed material and at sufficiently low densities to establish single molecular interactions.

The authors appreciate the major contributions by Andrew Leung and Susan Tha who developed the preparation procedures for ligand conjugation to the probe.

This work was supported by National Science and Engineering Research Council of Canada grant OGP155415, National Institutes of Health grant HL31579, and was stimulated by the program in *Science of Soft Surfaces and Interfaces* sponsored by the Canadian Institute for Advanced Research. R. Merkel is supported by a Feodor Lynen Fellowship from the Alexander von Humboldt Foundation.

REFERENCES

Ashkin, A. 1992. Forces of a single-beam gradient laser trap on a dielectric sphere in the ray optics regime. *Biophys. J.* 61:569–581.

Ashkin, A., K. Schutze, J. M. Dziedzic, U. Euteneuer, and M. Schliwa. 1990. Force generation of organelle transport measured in vivo by an infrared laser trap. *Nature.* 348:346–348.

Bell, G. I. 1978. Models for the specific adhesion of cells to cells. *Science.* 200:618–627.

Binnig, G., C. F. Quate, and C. H. Gerber. 1986. Atomic force microscopy. *Phys. Rev. Lett.* 56:930–933.

Drake, B., C. B. Prater, A. L. Weisenhorn, S. A. C. Gould, T. R. Albrecht, C. F. Quate, D. S. Cannell, H. G. Hansma, and P. K. Hansma. 1989. Imaging crystals, polymers, and processes in water with the atomic force microscope. *Science.* 243:1586–1589.

Evans, E. 1994. Physical actions in biological adhesion. *In* Handbook on Physics of Biological Systems, Vol. 1. R. Lipowsky and E. Sackmann, editors. Elsevier Science BV, Amsterdam. 697–728.

Evans, E., D. Berk, and A. Leung. 1991. Detachment of agglutinin-bonded red blood cells. I. Forces to rupture molecular-point attachments. *Biophys. J.* 59:838–848.

Evans, E., and K. Ritchie. 1994. Probing molecular attachments to cell surface receptors: image of stochastic bonding and rupture processes. *In* Scanning Probe Microscopies and Molecular Materials. J. Rabe, H. E. Gaub, and P. K. Hansma, editors. Kluwer Publishing, Amsterdam. In press.

Evans, E., and R. Skalak. 1980. Mechanics, and Thermodynamics of Biomembranes. CRC Press, Boca Raton, FL. 254 pp.

Hoh, J. H., J. P. Cleveland, C. B. Prater, J.-P. Revel, and P. K. Hansma. 1992. Quantized adhesion detected with the atomic force microscope. *J. Am. Chem. Soc.* 114:4917–4918.

Ishijima, A., T. Doi, K. Sakurada, and T. Yanagida. 1991. Sub-piconewton force fluctuations of actomyosin in vitro. *Nature.* 352:301–306.

Israelachvili, J. N., and G. E. Adams. 1978. Measurement of forces between two mica surfaces in aqueous electrolyte solutions in the range 0–100 nm. *J. Chem. Soc. Faraday Trans.* 174:975–1001.

Israelachvilli, J. N., and R. M. Pashley. 1982. The hydrophobic interaction is long range, decaying exponentially with distance. *Nature.* 300:341–342.

Israelachvilli, J. N., and R. M. Pashley. 1983. Molecular layering of water at surfaces and the origin of repulsive hydration forces. *Nature.* 306: 249–250.

Kishino, A., and T. Yanagida. 1988. Force measurements by micromanipulation of a single actin filament by glass needles. *Nature.* 334:74–78.

Kuo, S. C., and M. P. Sheetz. 1993. Force of single kinesin molecules measured with optical tweezers. *Science.* 260:232–234.

Leckband, D. E., J. N. Israelachvili, F.-J. Schmitt, and W. Knoll. 1992. Long-range attraction and molecular rearrangements in receptor-ligand interactions. *Science.* 255:1419–1421.

Lee, G. U., D. A. Kidwell, and R. J. Colton. 1994. Sensing discrete streptavidin-biotin interactions with atomic force microscopy. *Langmuir.* 10:354–357.

Luckham, P. F., and J. Klein. 1985. Interactions between smooth solid surfaces in solutions of adsorbing and non-adsorbing polymers in good solvent conditions. *Macromolecules* 18:721–728.

Maivald, P., H. J. Butt, S. A. C. Gould, C. B. Prater, B. Drake, J. A. Gurley, V. P. Elings, and P. K. Hansma. 1991. Using force modulation to image surface elasticities with the atomic force microscope. *Nanotechnology.* 2:103*a*. (Abstr.)

Marra, J., and J. Israelachvili. 1985. Direct measurement of forces between phosphatidylcholine and phosphatidylethanolamine bilayers in aqueous electrolyte solution. *Biochemistry.* 24:4608–4618.

Merkel, R., K. Ritchie, and E. Evans. 1995. Slow loading of biotin-streptavidin bonds yields unexpectedly low detachment forces. *Biophys. J.* 68:168s.

Parker, J. L., H. K. Christenson, and B. W. Ninham. 1989. Device for measuring the force and separation between two surfaces down to molecular separations. *Rev. Sci. Instrum.* 60:3135–3138.

Radmacher, M., R. W. Tillmann, M. Fritz, and H. E. Gaub. 1992. From molecules to cells: imaging soft samples with the atomic force microscope. *Science.* 257:1900–1905.

Radler, J., and E. Sackmann. 1992. On the measurement of weak repulsive and frictional colloidal forces by reflection interference contrast microscopy. *Langmuir.* 8:848–853.

Springer, T. A. 1990. Adhesion receptors of the immune system. *Nature.* 346:425–434.

Tees, D. F. J., O. Coenen, and H. L. Goldsmith. 1993. Interaction forces between red cells agglutinated by antibody. IV. Time and force dependence of break-up. *Biophys. J.* 65:1318–1334.

Tha, S. P., and H. L. Goldsmith. 1986. Interaction forces between red cells agglutinated by antibody. I. Theoretical. *Biophys. J.* 50:1109–1116.

Tha, S. P., J. Shuster, and H. L. Goldsmith. 1986. Interaction forces between red cells agglutinated by antibody. II. Measurement of hydrodynamic force of breakup. *Biophys. J.* 50:1117–1126.

van de Ven, T. G. M., and S. G. Mason. 1976. The microrheology of colloidal dispersions. IV. Pairs of interacting spheres in shear flow. *J. Colloid Interface Sci.* 57:505–516.

Zasadzinski, J. A. N., C. A. Helm, M. L. Longo, A. L. Weisenhorn, S. A. C. Gould, and P. K. Hansma. 1991. Atomic force microscopy of hydrated phosphatidylethanolamine. *Biophys. J.* 59:755–760.

Zilker, A., M. Ziegler, and E. Sackmann. 1992. Spectral analysis of erythrocyte flickering in the 0.3–4 μm^{-1} regime by microinterferometry combined with fast image processing. *Phys. Rev. A.* 46:7998–8001.